Seismic resilience evaluation of an urban overpass foundation

Juan M. Mayoral, Adriana Badillo & Mauricio Alcaraz
Institute of Engineering at UNAM, Mexico City, Mexico
Geotechnical and Structural Group - National Autonomous University of Mexico, Mexico City, Mexico

ABSTRACT
Resilience is the ability of a system to operate in a situation of extreme crisis and then to recover. In particular, seismic resilience evaluation of strategic infrastructure built in highly populated earthquake prone urban areas, such as Mexico City, is a key step to ensure earthquake preparedness actions. This paper describes the seismic resilience assessment of a critical support of a 23.5 km long urban overpass built in stiff soil, in the northeast Mexico City area. The evaluation was carried out considering both normal and subduction fault events expressed in terms of uniform hazard spectra for several return periods. Probabilistic site response analyses and site-specific numerically derived fragility curves were used to assess the critical support probability of failure, considering two foundation types: a conventional rectangular footing on piles foundation, and a so-called enhanced massive foundation. The seismic response of each foundation system was characterized using series of 3-D finite elements models developed with the program SASSI2000 for increasing seismic intensity levels. The effect of both soil conditions and ground motion characteristics on the structure-system response was accounted for in the analyses. The damage was defined in terms of earthquake induced lateral pier displacements, which was associated with column cracking, and loss of support of the upper deck. Finally, the increase on seismic resilience for the foundation alternative was established.

1 INTRODUCTION

Modern seismic design of strategic infrastructure such as metro lines, urban overpasses, life lines systems, or airports located in highly active earthquake areas, requires a proper seismic resilience assessment (Zio Enrico 2016) to foreseen the capacity of the system to withstand very large to extreme events, ensuring earthquake preparedness, and reducing life losses or post-earthquake distress. In particular, the large number of failures in bridges, viaducts and overpasses during large to extreme seismic events reported in the technical literature (Kazuhiko Kawshima 2011, Bray J. and Frost D. 2010 and Priestley et al. 1994) showed the importance of defining a proper approach to evaluate and, in turn, improve the seismic resilience of this type of structures. Seismic loading acting upon a soil-foundation system results from the interplay of earthquake incoming waves with the structure-swaying-produced waves, which in some cases may lead to an increase on the structural spectral ordinates in the foundation response with respect to those observed in the free field. Thus, resilience evaluations require a proper seismic risk assessment, in which potential structural damage is established for several ground intensities. From this evaluation, design improvements can be implemented. A key step in seismic risk analyses is the definition of an appropriate fragility function that captures the most important seismic failure modes of the overpass (Mayoral et al. 2016). A fragility function is a mathematical relationship that expresses the probability of reaching or exceeding a previously established limit or state of failure as a function of some measure of environmental excitation; usually a measure of acceleration, deformation, or force in an earthquake, hurricane or other extreme loading condition. From the practical standpoint, it is convenient to relate the probability of reaching or exceeding a given state of damage, with the peak ground acceleration in rock (PGA_{rock}). Thus, local codes can be used directly to estimate the probability of failure. Inhere, PGA_{rock} is related to lateral support column displacement, and, in turn, to the damage index. In this paper a novel methodology is applied to estimate the seismic resilience of strategic infrastructure aiming at enhancing its seismic performance. Similar approaches have been followed by other authors for specific cases such as retrofitted (Kim S and Shinozuka M. 2014), or isolated (Rezaul, K. R. and Yamazaki F. 2007) bridges.

2 CASE STUDY

As a case study, the seismic resilience evaluation of a critical support of a 23.5 km long urban overpass built in Mexico City is carried out. The location of the critical support within the overpass is presented in Figure 1. Site-specific fragility curves were obtained for two foundation alternatives: a) a 3.6 to 4.6 m^2 conventional rectangular footing on piles foundation, with concrete piles of 0.8m-diameter casted in-situ. The foundation is 1.70 m thick as shown in Figure 2, and b) an enhanced more resilient massive foundation, formed by adding concrete fill around the piles, up to a 6 m depth (Fig. 2b). A depth of 6.0 m was deemed appropriated based on the reduction of the expected spectral accelerations and the required relatively shallow excavation without support, which must be performed to place the massive enhancement. Considering the average undrained shear strength, s_u, of 40kPa to 50kPa, detected along the project, the critical excavation depth is about 7 m, assuming a safety factor of 2. Only those supports located in the critical zones, where number of blows corrected by energy and overburdening, $(N_1)_{60}$, are less than 15 in the upper 10 m,

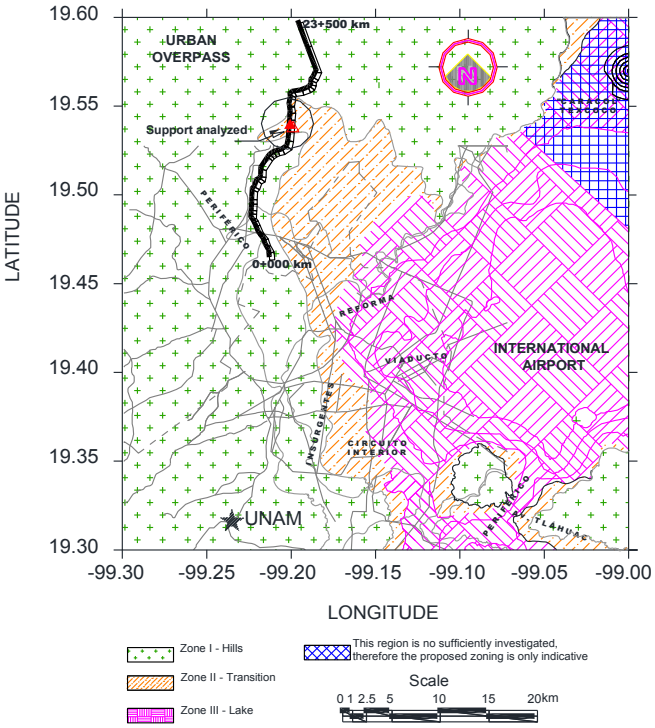

Figure 1. Urban overpass and studied supports locations

are to be strengthening. Since this technique requires only excavating a relatively narrow area around the pile cap foundation, prior placing the poor concrete filling, it represents a cost-effective alternative to be used to improve the seismic performance of both new and existing structures. Details on this foundation type were presented by Mayoral and Romo (2015). The overpass is comprised by an upper deck resting on top of central and support beams that are structurally tied to the columns, which, in turn, are monolithically attached to a rectangular foundation (Figure 2). The central beam is keep in place through bearings that are connected to the support beams. The methodology is applied to a specific support of the urban overpass to evaluate the foundation massive enhancement, thus the spatial ground motion variability along the overpass is not accounted for. However, the effect of this ground motion variability, due mostly to wave passage, loss of coherency and local site conditions, must be taken into account when analyzing the global overpass performance. These effects can substantially affect the fragility bridge response (Kim S.H. and Feng M.Q. 2003, Sextos et al. 2003).

3 METHODOLOGY

The proposed methodology is comprised by four main steps: 1) Seismic environment characterization, in which earthquake sources capable of producing damaging ground motions are identified, along with appropriate recurrence models and attenuation relationships, to develop uniform hazard spectra. For the case study presented herein, subduction and normal-fault events were considered, 2) Key failure modes identification and fragility curves derivation, inhering, lateral support displacement was selected as control variable, considering the fact that lateral displacement leads to loss of upper deck sitting, direct column structural damage, and eventually to bearing capacity failure. 3) Probability assessment of moderate to large damage using the fragility curves developed in step 2, and the results obtained from the seismic hazard carried out in step 1, and 4) Resilience evaluation through an appropriate index that accounts for the recovery time and potential loss of functionality, and its economic impact. Seismic resilience represents the ability of the infrastructure system to withstand an extreme event and to recover fast to a satisfactory functionality level. Usually, the resilience index is computed with the following expression (Karamlou A. and Bocchini P. 2015, Dong Y., and Frangopol D.M. 2015, Venkittaraman A. and Banerjee W. 2013):

$$R = \frac{\int_{t_0}^{t_0+t_h} Q(t)dt\bar{Q}}{t_h} \quad [1]$$

where R is the resilience index, t_0 is the time of occurrence of the extreme event, t_h is the investigated time considered, and $Q(t)$ is the time-variant functionality of the structure or system. For probabilistic resilience analysis, the expected functionality of the structure at each time instant t after an extreme event can be estimated by using an approach based on the total probability theorem. If a collection of events with a limited range of *IM*s is of interest, Equation [2] can be used to compute the expected functionality:

$$\bar{Q}(t) = \sum_{s=1}^{nIM} P(IM = s) \sum_{d=1}^{nDS} P(DS = d|\mathrm{IM} = s)Qd(t) \quad [2]$$

in which $Q_d(t)$ is the functionality recovery function of the structure at time t with an initial damage level d. This functionality is usually presented in the form of the

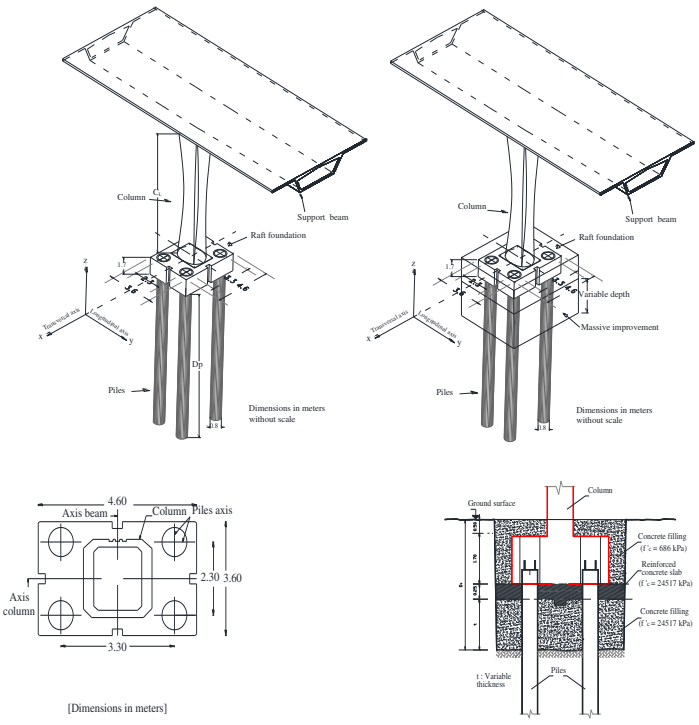

(a) (b)

Figure 2. Schematic representation of the support foundation for (a) conventional and (b) enhanced massive alternative

percentage of traffic-carrying capacity in normal conditions (HAZUS-MH 2004). $P(DS = d|IM = s)$ is computed from the fragility curves, and is the conditional probability of being in the damage state *d* given the event scenario with *IM* equal to *s*. Finally, $P(IM = s)$ is the probability of occurrence of extreme events generating intensity *s*, computed by a standard probabilistic seismic hazard analysis performed on the region where the system is located.

4 SEISMIC ENVIRONMENT CHARACTERIZATION

The urban overpass is located in a nearly flat area. To characterize the geotechnical subsoil conditions where the support is found, two standard penetration tests with selective undisturbed sample recovery were conducted. Cross hole CH-1 was performed to measure the shear wave velocity distribution with depth. This boring reached the so-called Tarango rock formation. Figure 3a shows the soil profile for the studied site. The groundwater table was not detected until the maximum explored depth. The soil profile at the support is comprised by a medium sandy silt and clay with intercalations of silty sand (i.e. undrained shear strength, s_u, of 43kPa), which extends down to 11 m. After this depth and down to 23 m, there is dense to medium silty sand with sandy silt intercalations. Underlying this formation, and down to the maximum explored depth, there is a very dense sandy silt and silty sand layers with gravels (i.e. $(N_1)_{60}$, larger than 60). The water content in the sandy and silty materials is about 20%. Shear wave velocity measurements as a function of depth for the site are presented in Figure 3b. Small strain shear modulus G_{max} (for strain levels of 10^{-5} or less) were determined directly from the measured shear wave velocity, V_s. Due to the lack of experimental information regarding the soil dynamic properties of the materials found at the site, these were estimated based on the normalized modulus degradation and damping curves proposed by Vucetic and Dobry (1991) for clays, as a function of plasticity index, (PI), considering the information gathered from index properties. Regarding the sand and silt layers, the curves proposed by Seed and Idriss (1970) were deemed appropriated. Both sets of curves are presented in Fig. 4.

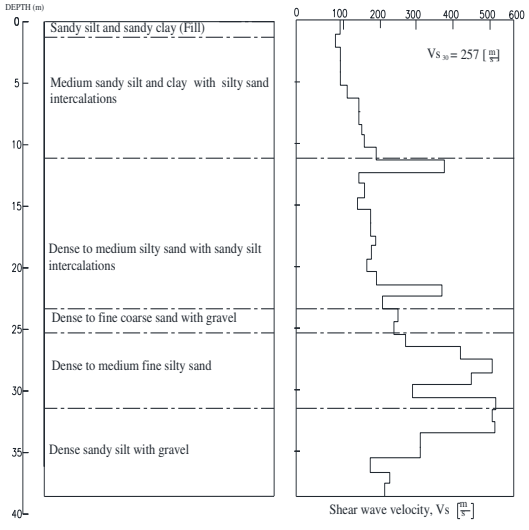

(a) (b)

Figure 3. (a) Subsurface conditions at the studied site and (b) shear wave velocity profile at site

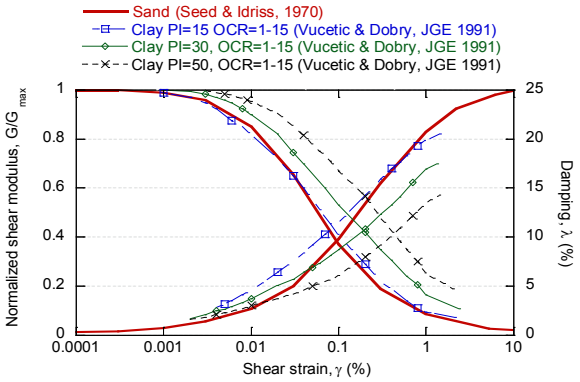

Figure 4. Normalized shear stiffness and damping curves used in the analyses

4.1 Uniform hazard spectrum

The uniform hazard spectrum in rock determined to characterize the seismic environment was developed at UNAM, at about 20 km from the site, to be able to compare it directly with measured responses, if needed, for future earthquakes. As it is well known, the uniform hazard spectra, UHS, is a representation of the relationship between the natural vibration period, T, and spectral acceleration, Sa, for a given exceedance probability associated with a return period. Uniform hazard spectra for four return periods (i.e. 125, 250, 475 and 2475 years) were obtained from the seismic hazard curves for both normal and subduction fault events, as depicted in Figure 5.

4.2 Probabilistic site response analysis

Probabilistic site response analyses were carried out using random vibration theory. The algorithm used to compute the probabilistic site response of horizontally stratified soil deposits subject to two dimensional SH waves propagating vertically is formulated in the frequency domain, assuming equivalent linear soil properties. It uses the Thompson–Haskell (1953) solution. The input motion is defined in terms of a response spectrum from which the equivalent power spectrum of the excitation is computed. The accelerations, strains and response spectra in different points of the system are computed from the corresponding power spectrum and the extreme value theory. Thus, this random process is completely characterized by its power spectra. Using the random vibration theory, the maximum responses of a linear system excited by a stochastic process can be computed for a given confidence level. Physically this characterization of the seismic environment is equivalent to consider an infinite number of acceleration time histories with the same mean frequency content but with randomly distributed phases. The computed response spectra for the site and seismogenic zones are presented in Figure 6. The results from both the hazard and probabilistic site response analysis are to be used only in the application demonstrated in Table 5.

5 FRAGILITY CURVES DEVELOPMENT

Site-specific fragility curves were obtained following the approach described in Mayoral et al. (2016), for both foundation types, conventional and enhanced massive foundation. As previously described, the conventional 3.6 to 4.6 m^2 foundation is structurally connected to concrete piles of 0.80 m diameter casted in-situ. The mat foundation is 1.70 m thick as shown in Figure 2. The enhanced, more resilient massive foundation, is formed by adding concrete fill around the piles, up to a 6m depth (Figure 2b). The geometry, material properties, and structure details are parameters that describe the typology of the urban overpass and its capacity to withstand seismic loads. The seismic loads are function of the surrounding soil, seismic environment and the soil–structure interaction. The selection of the seismic input motion is also essential in the seismic response analysis of the soil–structure system.

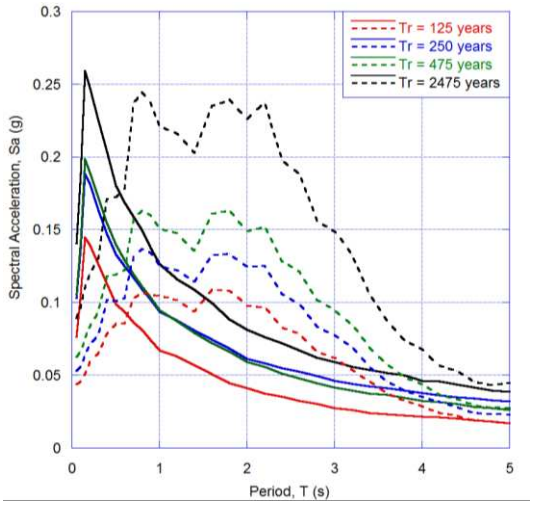

Figure 5. Uniform hazard spectra for Tr=125, 250, 475 and 2475 years for subduction (dotted line) and normal (solid lines) events

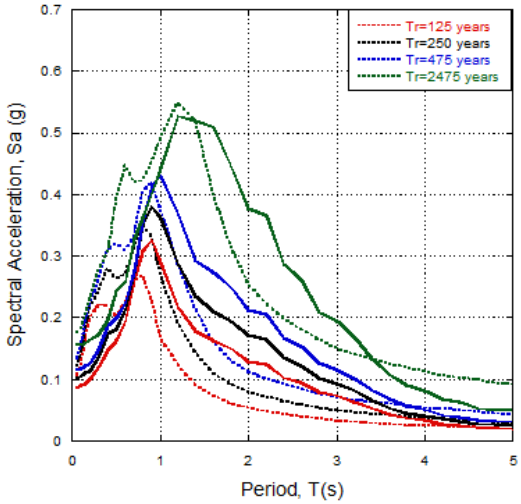

Figure 6. Response spectra at the ground surface for the site for subduction (solid line) and normal (dotted line) events

Different ground motions were selected based on amplitude, frequency content and duration. Damage is quantified in terms of the maximum lateral column displacement normalized by the column height, and is related to peak ground acceleration in rock PGA_{rock}. Finally, fragility curves are derived for different damage states (minor, moderate and extensive) considering the primary sources of uncertainties

5.1 Numerical study

A numerical study was conducted in order to characterize the damage that each support typology can exhibit for several seismic shaking scenarios varying from moderate to extreme ground shaking. Ground conditions corresponds to type C, according to the Eurocode (2004). The selected ground motions were based on spectrum matching using the EC8 spectrum to ensure that the numerically derived fragility curves are representative of a wider variety of seismogenic zones, thus facilitating its application in engineering practice. The corresponding soil profile and shear wave velocity distribution with depth considered is presented in Figure 3b. Both normal and subduction fault events were considered. Table 1 summarizes the seismic events used in the analyses. A total of eight ground motions recorded during these events were selected, which exhibits a wide range of spectral acceleration amplitudes, frequency content, significant duration and seismotectonic environment. These ground motions were recorded either at rock or firm soil. Figure 7 presents the response spectra of the selected motions together with the EC8 spectrum for soil class A, normalized with respect to their corresponding PGA. The time histories are scaled to five intensity levels of PGA on rock (i.e. 0.15, 0.30, 0.45, 0.60 and 0.75 g) in order to calculate in the dynamic analyses the response of the urban overpass system to an increasing seismic excitation. Thus, 25 cases were analyzed for each foundation configuration.

5.2 Numerical model

Sets of 3D finite element models of the soil-foundation structure system were developed with the computer program SASSI2000 (2000), using the flexible volume method. The soil-structure system was divided into the soil, the foundation and the structure. For the analyses presented herein, the structure was modeled with three dimensional beam elements and lumped masses, the foundation with 3-D brick finite elements, and the piles with three dimensional beam elements and excavated soil with rigid links, to account for pile diameter effects. This approach allows capturing this effect approximately using the three dimensional beam elements available in SASSI2000.

Table 1. Earthquakes considered in the analyses

Seismogenic Zone	Earthquake Name	Year	Moment magnitude, M_w	Epicentral distance, R (km)	PGA (m/s^2)	Duration (sec)
Normal	Montenegro (former Yugoslavia)	1979	6.9	21	1.7	47.9
	Kocaeli (Gebze, Turkey)	1999	7.4	42	0.2	32
	Umbria Marche (Gubbio-Piana, Italy)	1998	4.8	18	0.2	40
Subduction	Maule (Concepcion San Pedro, Chile)	2010	8.8	109.1	0.6	120
	Honshu (Haga, Japan)	2011	9	282.8	0.8	300
	Michoacan (Tacubaya, Mexico)	1985	8.1	395.6	0.032	170

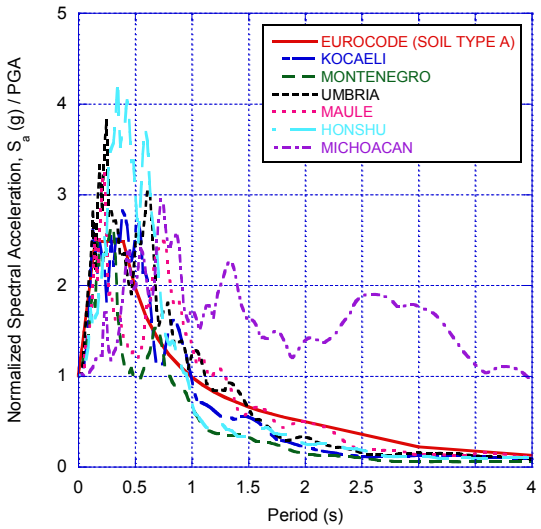

Figure 7. Response spectra for selected input motions and Eurocode 8

Finally the soil was considered as axis-symmetric, and comprised by series of semi-infinite viscoelastic horizontal layers with equivalent linear properties (i.e. shear stiffness and damping) resting on top of a viscoelastic half-space. The foundation-structure interaction occurs at all basement nodes. The half-space transmitting boundary was used at the edges of the models to simulate the pga field conditions. To guaranty a good estimation of the structure performance, it is necessary the calibration of numerical models, such as those developed with finite elements or finite differences, which allows the simulation of ground, foundation, and structure. For instance, several researches have reported to be able to predict the seismic response of bridges using SASSI (e.g. Ganev et al. 1998 and Mayoral et al. 2009). Series of equivalent-linear properties, which depend on the shear strain level associated to each PGA_{rock} considered and seismogenic zone, were derived with the program SHAKE (Schnabel et al. 1972), and used in the SASSI analyses. These properties were deemed appropriate to approximate the soil non-linearity, considering that in the cases studied herein the high stiffness of the soils will preclude the generation of important shear strains.

5.3 The substructure model

The piles were modeled with three-dimensional beam elements plus excavated soils and rigid links, and the massive pile cap with three-dimensional (3-D) solid elements (Ganev et al. 1998). The excitation was assumed acting in the transverse component. The substructure damping was characterized through a Rayleigh type formulation (i.e. mass and stiffness dependent damping). Due to the presence of the massive pile cap, no gapping between the foundation and the soil was expected to develop. The beam elements are connected directly to the soil elements at the nodes of the excavated soil with rigid links, transmitting both strains and stresses. The potential cracking of the piles was not considered, because as design requirement the piles must work in their elastic range. The total mass of the upper deck and support beam was concentrated in three lumped masses to distribute the upper deck inertia, and connected by rigid members to the beams elements that represent the columns, which in turn, were simulated with eleven beam elements. This allows modeling potential rocking of the overpass deck. This assumption was based on the fact that, for the cases studied herein, the support beam, and the deck are structurally tied to the column. The structure, including the column and upper deck were pre-stressed and made of high strength concrete, as presented in Table 2. Thus, for the column and the rectangular footing pile foundation it was considered a Young's modulus of 30,000 MPa, a Poisson ratio of 0.3, a unit weight of 23.5 kN/m3 and a damping ratio of 3%. The structure damping was modeled with a Rayleigh type formulation and a viscous boundary at base was considered (i.e. flexible base condition). This boundary consists of two dashpots per unit area of the boundary. For the concrete filling, it was assumed a Young's modulus of 19,400 MPa.

5.4 Damage index and damage states

An accurate estimation of the support beams displacements, in both the transversal and horizontal components must be carried out to ensure that relative movements between them will not trigger a separation of the central and the support beam. Thus, the probability of collapse of the upper deck will be reduced. For this research, the damage index, DI, was established based on the column lateral displacement normalized by an average column height (i.e. 10m). Following the criteria presented by Franchetti et al. (2004), considering the cracking strain defined from a pushover test carried out by Muria et al. (2015), four different damage states were established. These refer to minor, moderate, extensive and complete damage of the urban overpass, as presented in Table 3. A DI larger than 0.006 corresponds to a lateral column displacement larger than 6 cm approximately, which exceeds the initial column cracking displacement (i.e. 1 cm) about 6 times according to the lateral load-displacement field test performed in the urban overpass bridge support as reported by Muria et al. (2015). This strain level is related to severe column structural damage, as well as potential loss of beam sitting and damage in the seismic stops.

Table 2. Concrete strength of structural elements

Structural element	$f'_c\ (kPa)$
Reinforced concrete slab	24,500
Piles	24,500
Fluid filling	24,500
Prefabricated columns and rectangular footing pile foundations	59,000
Fluid filling for the excavation	686

Table 3. Definition of damage states for urban overpass

Damage state (dsi)	ds0. None	ds1. Minor/slight	ds2. Moderate	ds3. Extensive	ds4. Complete
Range of damage index	DI ≤ 0.002	0.002 < DI ≤ 0.003	0.003 < DI ≤ 0.004	0.004 < DI ≤ 0.006	DI > 0.006

5.5 Derivation of fragility curves

For structural damage, given the displacement, associated to an expected PGA in rock, the probability of being in or exceeding a damage state, d_s, is modeled as:

$$F_i(PGA) = \Phi\left(\frac{ln^{PGA}/_{PGAm_i}}{\beta tot}\right) \quad [4]$$

where Φ is the standard cumulative normal distribution, PGA_{mi} is the median threshold value of the earthquake intensity measure, required to cause the ith damage state and β_{tot} is the total lognormal standard deviation. Therefore, the development of fragility curves according to Eq. [4] requires the definition of the medians PGA_{mi} for each damage state and the value of β_{tot}. The latter describes the total variability associated with each fragility function, commonly including three sources of uncertainty (HAZUS-MH 2004): the definition of damage states (β_{ds}), the response and resistance (capacity) of the element (β_C), and the variability in the earthquake input motion (demand) (β_D). In the present study, due to the lack of a rigorous estimation, β_{ds} is set equal to 0.4 following HAZUS (2004) approach, β_C is considered equal to 0.4 as presented by Franchetti et al. (2004), while β_D is estimated based on the variability in urban overpasses response (DI) that have been calculated for the different ground motions. The value of β is estimated as the root of the sum of the squares of the component dispersions. The median threshold value of the earthquake parameter, PGA_{mi} is obtained for each damage state based on the evolution of damage with increasing earthquake intensity. The corresponding fragility curves are illustrated in Figure 8 for both foundation types. The parameters of the numerically-derived fragility curves are summarized in Table 4. The fragility curves were developed based on the peak ground acceleration determined on rock, PGA_{rock}, located nearby a given project site for both subduction and normal-fault events scaled up to 0.75g of PGA_{rock}.

Evidently, the derived fragility curves can be applied for preliminary purposes only to cases where the bridge foundation, soil conditions and seismic environment are similar to those considered in the analyses. Comparing the fragility curves for each foundation, conventional and enhanced, it can be clearly noticed the benefits of the second option, in which the probability of damage is substantially reduced (i.e. about 60 % for small PGA_{rock}, and up to 20 % for medium to large PGA_{rock}).

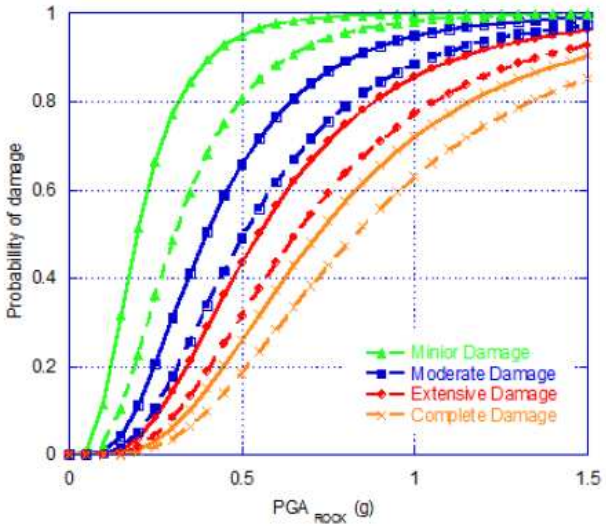

Figure 8. Fragility curves for conventional (solid lines) and enhanced massive (dashed lines) foundation

Table 4. Parameters of the numerical fragility curves for urban overpass

Ds	Conventional		Enhanced	
	Median PGA_{rock} (g)	β_{tot}	Median PGA_{rock} (g)	β_{tot}
Minor	0.20	0.57	0.31	0.57
Moderate	0.40	0.57	0.51	0.57
Extensive	0.55	0.57	0.66	0.57
Complete	0.72	0.57	0.83	0.57

6 RESILIENCE ASSESSMENT

Based on the site-specific fragility curves developed herein, and the results gathered from the probabilistic site response analysis, the seismic resilience evaluation of the critical support of the urban overpass was conducted, computing the actual probability of failure for each case. Table 5, presents the corresponding results. It can be clearly noticed that the probability of failure is reduced when using the enhanced foundation. The percentage of improvement goes from 60% to 50% for the critical cases. Regarding the seismic resilience, the conditional probability of being in the damage state *d* given the event scenario with *IM* equal to *s* was computed based on the numerically-derived fragility curves of conventional and enhanced foundations. Due to the lack of data, the functionality recovery functions of the structure proposed in HAZUS (2004) for urban bridges was used in the resilience index computation.

Table 5. Probability of damage for the critical support

Seismogenic Zone	Period Return	PGA_{rock} (g)	Probability of Damage (%)							
			Conventional Foundation				Enhanced Foundation			
			Mi[1]	Mo[2]	E[3]	C[4]	Mi[1]	Mo[2]	E[3]	C[4]
Normal	125 years	0.119	20.8	2.1	0.3	0.1	5.9	0.7	0.1	0.0
	250 years	0.155	31.6	4.2	1.1	0.3	10.4	1.6	0.5	0.1
	475 years	0.171	41.4	7.7	2.4	0.7	16.6	3.3	1.1	0.4
	2475 years	0.220	58.9	15.9	6	2.1	29.4	7.8	3.1	1.1
Subduction	125 years	0.105	11.6	0.7	0.1	0	2.4	0.2	0.0	0.0
	250 years	0.122	21.6	2.5	0.6	0.2	6.4	0.9	0.2	0.1
	475 years	0.138	22.1	3.1	0.9	0.4	7.0	1.3	0.3	0.1
	2475 years	0.172	41.4	7.7	2.4	0.7	16.6	3.3	1.1	0.4

[1]Minor; [2]Moderate; [3]Extensive; [4]Complete

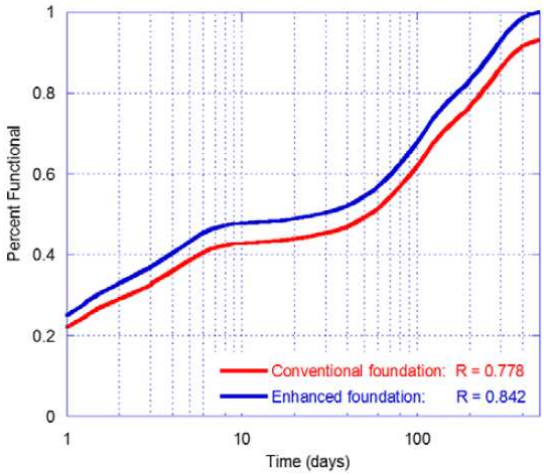

Figure 9. Expected functionality curves for the critical support

The probability of occurrence of extreme events generating intensity *s*, was obtained from the probabilistic seismic hazard analysis. The computed expected functionality functions are presented in Figure 9, along with their resilience index, R. Seismic resilience after the enhancement increases up to 8% for an investigated time t_h of 497 days.

7 CONCLUSIONS

Seismic resilience evaluation of strategic infrastructure is a mandatory step to reduce both material losses and human causalities after a major earthquake, and improve seismic resilience at the community level. This paper describes the application of a novel methodology to assess seismic resilience, and quantify seismic design performance enhancement, of critical infrastructure systems. The approach is comprised of four steps: 1) Seismic environment characterization, 2) Key failure modes identification and fragility curves determination, 3) Probability assessment of moderate to large damage, and 4) Resilience assessment and design enhancement. For the case study included herein, an increase on seismic resilience up to 8% was achieved for critical supports of an urban overpass, going from a conventional to an enhanced massive foundation. Site-specific fragility

curves for urban overpasses built in stiff soils were generated (i.e. soil type c according to Eurocode (2004)). The proposed procedure allows both to characterize the seismic performance of the original foundation design, and provides a rational way of estimating resilience improvement by enhancing the original seismic design. More accurate information regarding recovery times of urban overpasses located in heavily populated urban areas, after major to extreme earthquake events, such as Mexico City, is needed to better characterize these recovery functions, especially considering the strong dependency of the resilience index R with the recovery time distribution expressed through the restoration curves.

8 REFERENCES

Zio Enrico, 2016. Challenges in the vulnerability and risk analysis of critical infrastructures. Reliability Engineering and System Safety 152.137–150.

Kazuhiko Kawshima. Damage of bridges resulting from fault rupture in the 1999 Kocaeli and duzce, Turkey earthquakes and the 1999 Chi-Chi, Taiwan earthquake. In proceedings of Seismic Fault-induced Failures, Tokyo Institute of Technology, 2001, pp 171-190.

Bray J. and Frost D. (Editors), 2010, Geo-engineering reconnaissance of the 2010 Maule, Chile earthquake, Report of the NSF sponsored GEER association team No. GEER-022.

Romo, M. P., 1995 Clay behavior, soil response and soil structure interaction studies in Mexico City. In: Proceedings of the third international conference on recent advances in geotechnical earthquake engineering and soil dynamics, vol 2. San Luis Missouri, USA. 1039–1051.

Mayoral, J.M., Argyroundis S., and Castañon, E., 2016. Vulnerability of floating tunnel shafts for increasing earthquake loading. Soil Dynamics and Earthquake Engineering 80. 1–10

Kim, S-H and Shinozuka M., 2014 Development of fragility curves of bridges retrofitted by column jacketing. Probabilistic Engineering Mechanics 19 (2004) 105–112

Rezaul, K. R., and Yamazaki F. Effect of isolation on fragility curves of highway bridges based on simplified approach. Soil Dynamics and Earthquake Engineering 27 (2007) 414–426

Mayoral, J.M and P. Romo. Seismic response of bridges with massive foundations. Soil Dynamics and Earthquake Engineering 71 (2015) 88–99

Kim SH, and Feng MQ (2003). Fragility analysis of bridges under ground motion with spatial variation. Int J Nonlinear Mech, 38(5):705-21.

Sextos A, Pitilakis K, and Kappos A (2003). Inelastic dynamic analysis of RC bridges accounting for spatial variability of ground motion, site effects and soil-structure interaction phenomena. Part 1: Methodology and Analytical tools, Earthquake Engineering and Structural Dynamics 32(4): 607-627.

Karamlou A, and Bocchini P (2015) Computation of bridge seismic fragility by large-scale simulation for probabilistic resilience analysis, Earthquake Engineering & Structural Dynamics, DOI: 10.1002/eqe.2567.

Dong Y, and Frangopol DM (2015) Risk and resilience assessment of bridges under mainshock and aftershocks incorporating uncertainties, Engineering Structures, 83, 198-208.

Venkittaraman A, and Banerjee W (2013) Enhancing resilience of highway bridges through seismic retrofit, Earthquake Engineering & Structural Dynamics, DOI: 10.1002/eqe.2392

NIBS. HAZUS-MH: technical manuals. Washington, DC: Federal Emergency Management Agency and National Institute of Building Science; 2004.

Vucetic M, and Dobry R. Effect of soil plasticity on cyclic response. J Geotech Eng 1991; 114(1):89–107.

Seed HB, and Idriss I M. Soil moduli and damping factors for dynamic response analysis. (UCB/EERC-70/10).Berkeley: University of California;1970.

Osorio L, Mayoral J M. Seismic microzonation for the northeast Texcoco lake area, Mexico. Soil Dyn Earthq Eng 2013; 48 (2013): 252–66.

Thomson-Haskell NA. The dispersion of surface waves on multilayered media. Bulletin of the Seismological Society of America 1953; 43:17–34.

EC8 (2004). Eurocode 8: Design of Structures for Earthquake Resistance. Brussels, Belgium: European Committee for Standardisation; The European Standard EN 1998-1.

Lysmer J, Ostadan F, Tabatabaie M, Tajirian F, and Vahdani S. SASSI A system for analysis of soil-structure interaction. CA: University of Berkeley; 2000.

Lysmer J. Analytical procedures in soil dynamics. (ReportNo.EERC78/29). Berkeley: University of California; 1978(December).

Mayoral Juan M., Flores Francisco A, and Miguel P Romo. Seismic response evaluation of an urban overpass. Earthq Eng Struct Dyn 2011; 40:827–45.

Ganev, T., Yamazaki, F., Ishizaki, H., and Kitazawa, M. 1998 “Response analysis of the Higashi-Kobe Bridge and surrounding soil in the 1995 Hyogoken-Nanbu Earthquake”, Earthquake Engineering & Structural Dynamics Volume 27, Issue 6, Date: June, Pages: 557-576.

Mayoral J.M., Alberto Y, Mendoza M.J, and Romo MP. Seismic response of an urban bridge-support system in soft clay. Soil Dyn Earthq Eng 2009; 29(5):925–38.

Schnabel PB, Lysmer J, and Seed HB. SHAKE: a computer program for earthquake responser analysis of horizontally latered sites. CA: College of Engineering, University of Berkeley; 1972 (Rep., No.EERC72-12).

P. Franchetti, M. Grendene, C. Modena, D. Slejko, and F. Bergo. Evaluation of seismic risk: application to bridges and viaducts in veneto (Italy). 13th World Conference on Earthquake Engineering. Vancouver, B.C., Canada. August 1-6, 2004. Paper No. 2791.

Murià-Vila, D., Sánchez-Ramírez, A.R., Huerta-Carpizo, C.H., Aguilar, G., Pérez, and J.C., Carrillo Cruz, R.E. Field tests of elevated viaducts in Mexico City. Journal of Structural Engineering (United States) Volume 141, Issue 1, 1 January 2015, Article number D4014001